CrossMark

Effects of annealing temperature on structure and electrical properties of (Na, K)NbO₃ thin films grown by RF magnetron sputtering deposition

Jiewen Huang[1] · Jinsong Liu[1,2] · Ziquan Li[1,3] · Kongjun Zhu[2] · Bijun Wang[1] ·
Qinlin Gu[2] · Bing Feng[1] · Jinhao Qiu[2]

Abstract In this study, lead-free (Na, K)NbO₃ films were successfully deposited by RF magnetron sputtering and subsequent annealing treatment, in which a KNN atmosphere was projected to prevent the alkali metal volatilization. Effects of annealing temperatures on structure and electrical properties of the KNN thin films were investigated systematically. The results show that, with the temperature increasing, the KNN films started crystallization accompanying with volatilization of alkaline elements as well as phase transition. The particle size and surface quality of the film closely depended on annealing temperature and atmosphere. The (100) preferred orientation, large grain size, dense morphology, and annealing atmosphere all benefited the electrical properties of the KNN films. Notably, the KNN films deposited at 200 °C and subsequent annealed at 650 °C showed a well polarization of $2P_r = 20.8$ μC/cm² and coercive field $2E_c$ of 200 kV/cm.

1 Introduction

With the legislation restricting the utilization of lead-based materials, the KNN-based thin films have been paid much attention. To date, it has been generally accepted that (K, Na)NbO₃ (KNN)-based films are the most promising candidate materials because of high piezoelectric properties and high Curie temperatures. As a result, numerous techniques have been conducted to fabricate high-quality KNN films, including pulsed laser deposition [1, 2], RF magnetron sputtering [3], chemical solution deposition method [4], sol–gel processing [5], and so on. However, the volatilization of the alkali metal elements was still a disadvantage in crystallization process of KNN films, which made it difficult to fabricate the high-quality films.

Recently, many effects have been made to preserve the alkali metal elements in the films. For example, Li and Sun [6, 7] found that the optimal excess value of K and Na could largely decreased the Na, K and oxygen vacancies, and improve electrical properties of KNN films. Meanwhile, the introduction of Li, Ta, Co, and Mn [8–12] into KNN films played an important and indispensable role in enhancing ferroelectric and piezoelectric properties of the films. Adding V₂O₅ or Nb₂O₅ seed layers with different thickness were also found to reduce the crystallization temperature, and prevent alkali metal volatilization and thus largely improve microstructure and leakage property [13, 14]. In addition, subsequent annealing treatment in KNN atmosphere was thought to be a key for high-quality KNN thin films with good ferroelectric properties [15].

Compared with compositional modification, optimizing annealing temperature seems to be a simpler and easier pathway for improving electrical properties of KNN films [16]. However, there is little report on the effects of annealing temperature on the microstructural and electrical properties of KNN films derived from RF magnetron sputtering method, which is one of the suitable routes to make high quality and uniform films on large area substrate. In this study, we obtained high quality KNN thin films prepared by RF-magnetron sputtering and subsequent

✉ Jinsong Liu
 jsliu@nuaa.edu.cn

1 Department of Materials Science and Technology, Nanjing University of Aeronautics and Astronautics, Nanjing 210016, Jiangsu, China

2 State Key Laboratory of Mechanics and Control of Mechanical Structures, Nanjing University of Aeronautics and Astronautics, Nanjing 210016, Jiangsu, China

3 Chemical Engineering Department, Nanjing College of Chemical Technology, Nanjing 210048, Jiangsu, China

annealing treatments in KNN atmosphere, and influence of annealing temperature on the structural and electrical properties of KNN films was systematically investigated.

2 Experimental details

All of the KNN thin films were deposited at $Pt/Ti/SiO_2/$ $Si(100)$ substrates by radiofrequency (RF) magnetron sputtering using a stoichiometric target (diameter: 60 mm). Deposition of the KNN thin films was carried out at 200 °C in a mixed argon and oxygen ($Ar:O_2 = 4:1$) atmosphere with a total pressure of 1.3 Pa and a constant power of 90 W. Annealing treatment was performed at various temperatures of 600–800 °C for 1 h in KNN atmosphere after the mixed powder of Na_2CO_3 and K_2CO_3 was raised to 800 °C along with the furnace and kept for 30 min.

The crystal structure and morphology of the as-prepared KNN films were examined by using X-ray diffraction (Rikagu UltimaIV) and scanning electron microscopy (s4800 field-emission scanning electron microscope, respectively. And the electrical properties of the films were measured in a vertical capacitor structure, with Au deposited on the KNN films as the top electrode by using conventional DC sputtering. The polarization–electric field (P–E) hysteresis loop was measured by a ferroelectric tester (TF Analyzer 2000).

3 Results and discussion

The crystallinity and phase of the films were confirmed by X-ray diffraction. XRD patterns of the KNN films annealed at different temperatures and bulk KNN ceramic are shown in Fig. 1. It's observed that the thin film annealed at 600 °C was amorphous with no peaks appeared. Whereas, the films annealed at 650 °C exhibited distinct crystal state with single perovskite phase of KNN devoid of any secondary phases. The pronounced diffraction peaks at $2\theta = 22.3°$, $31.7°$, $46.2°$, $51.5°$ and $56.6°$ correspond to the five crystal plans of (100), (110), (200), (210) and (211), respectively. The crystallization of the films annealed at 700 °C was further improved, accompanying with the increasing intensity of diffraction peaks. However, when the temperature reached to 750 °C, the intensity of peaks became weaker, which may come from the volatilization of alkaline elements [17] as well as phase transition [18]. The obvious splitting of (002)/(200) at $2\theta = 46°$ and (001)/(100) at $2\theta = 22.4°$ doubles occurred at 800 °C, which indicated that the KNN thin film transformed from a orthorhombic into tetragonal [19–21].

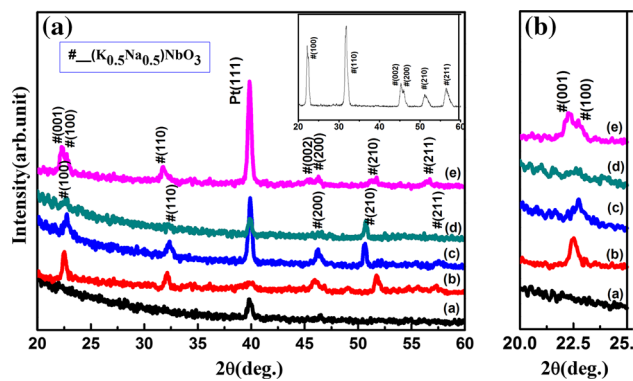From Fig. 1a, for the KNN ceramic, the intensity of the (110) reflex was highest. However, the intensity of (100)

Fig. 1 a The XRD patterns of KNN films annealed at different temperatures: (*a*) 600 °C; (*b*) 650 °C; (*c*) 700 °C; (*d*) 750 °C; (*e*) 800 °C and the *inset* shows the XRD pattern of bulk KNN ceramic. **b** The enlarged view between $2\theta = 20°–25°$ in (**a**)

peak was higher than that of (110) peak for all the deposited films. In order to evaluate the degree of the crystallographic orientation of the KNN ceramic and the films, the intensity ratios of the (100) to the (110) reflex were calculated by Eq. (1) in the following form:

$$P = \frac{\int I_{100}}{\int I_{110}}. \tag{1}$$

Here the p represents the intensity ratio of the (100) to the (110) reflex. $\int I_{100}$ and $\int I_{110}$ refer to the integrated intensities of the (100) and the (110) peaks respectively. As Table 1 shows, for the KNN ceramic, the intensity ratio of the (100) to the (110) reflex was calculated to be about 0.65. However, for all the KNN films, the intensity ratios of the (100) to the (110) reflex were all larger than 1, which showed more or less pronounced (100) preferential orientation. The intensity ratios decreased from 1.67 for the sample annealed at 650 °C to 1.30 for the sample annealed at 700 °C, and then increased from 1.40 for the sample annealed at 750 °C to 1.92 for the sample annealed at 800 °C. The changing trend of the intensity ratios of the (100) to the (110) reflex with the increasing temperature was very similar to that of interplanar spacing.

Table 1 Lattice parameter and intensity ratio of the (100) to the (110) reflex for KNN ceramic and films annealed at different temperatures calculated from XRD measurements

Sample	a (nm)	(100)/(110)
600 °C	–	–
650 °C	0.3943	1.67
700 °C	0.3908	1.30
750 °C	0.3928	1.40
800 °C	0.3990	1.92
KNN ceramic	0.4003	0.65

From Fig. 1b it can be seen that, when the temperature reached to 700 °C, the (100) peaks of the films shifted towards higher angle compared with that of the films annealed at 650 °C. However, when the temperature reached above 700 °C, the (100) peaks of the films shifted towards lower angles, leading to the changing of lattice constant. Based on Bragg's equation (Eq. 2) and d-spacing equation for orthorhombic (Eq. 3) and tetragonal (Eq. 4) structures,

$$2d \sin \theta = n\lambda. \tag{2}$$

$$1/d^2 = h^2/a^2 + k^2/b^2 + l^2/c^2. \tag{3}$$

$$d = \frac{a}{\sqrt{h^2 + k^2 + l^2 \left(\frac{a^2}{c^2}\right)}}. \tag{4}$$

the results in Table 1 show that the lattice parameters decreased from 0.3943 nm for the sample annealed at 650 °C to 0.3908 nm for the sample annealed 700 °C,

Fig. 2 SEM surface (**a** 600 °C, **b** 650 °C, **c** 700 °C, **d** 750 °C, **e** 800 °C) and cross-sectional morphologies (**f** 650 °C, **g** 800 °C) of KNN thin films annealed at different temperatures, and curves of the average diameter of grains under different annealing temperatures (**h**)
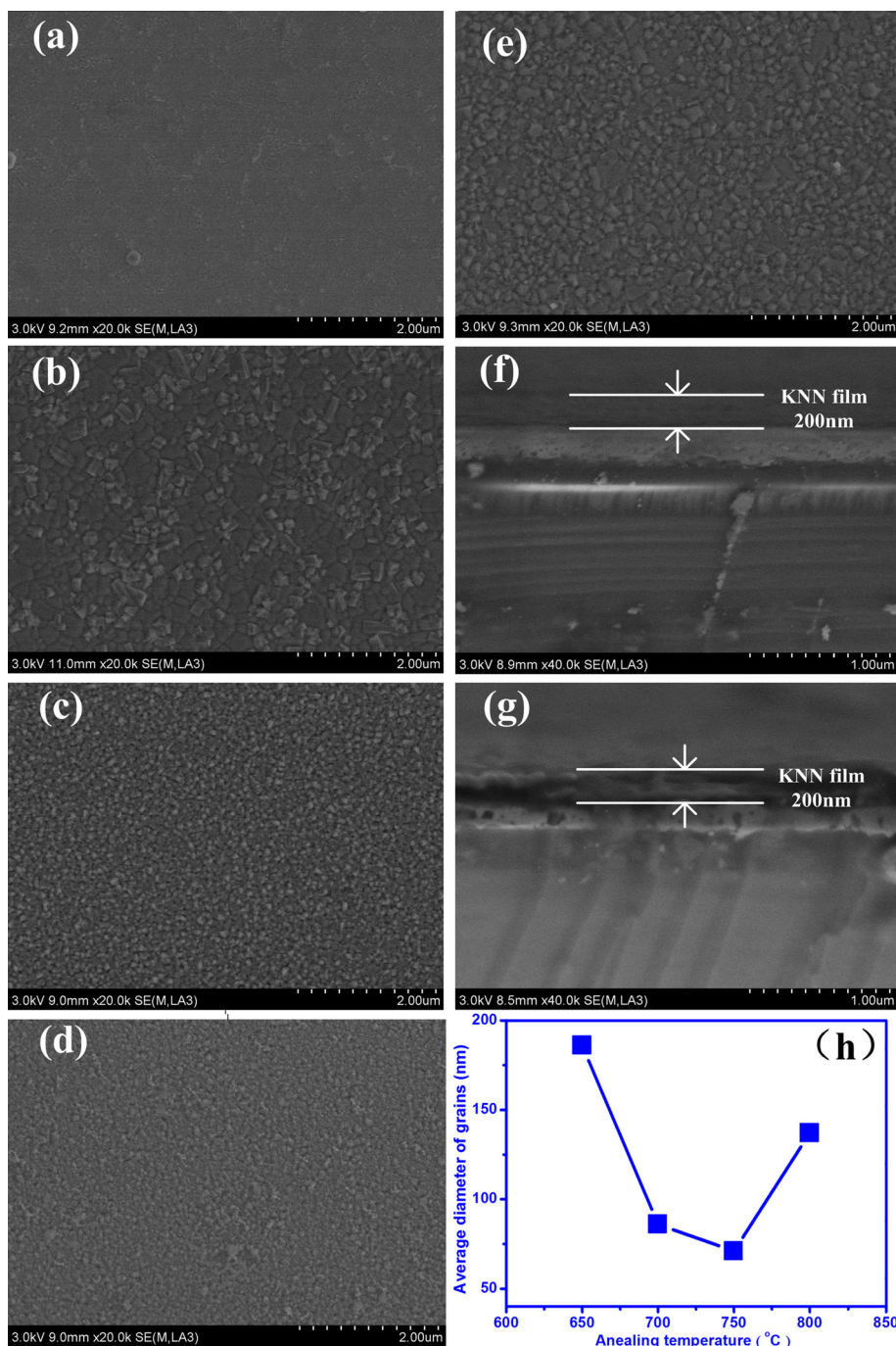
which may be related to the increasing internal stress in the orthorhombic film at low temperature. However, after the films changed to tetragonal structure, the lattice parameters increased from 0.3928 nm for the sample annealed at 750 °C to 0.3990 nm for the sample annealed at 800 °C, and the increasing interplanar spacing with increasing temperature may be caused by the strains relaxation in the films at high temperature. With comparison to the bulk KNN ceramic (a = 0.4003 nm, seen in Table 1), there were always the strains in the KNN films, and the inevitable stress was often induced by the lattice mismatch and the difference of the thermal expansion between the films and the substrate as Tanaka et al. [17] reported.

The surface and cross-sectional morphologies of the thin films annealed at different temperatures were presented in Fig. 2. The KNN film annealed at 600 °C displayed a uniform surface and no crystal grains were observed (Fig. 2a). As the temperature reached to 650 °C, the clearly observed gains suggested the beginning of crystallization. The average diameter of grains continually changed with increasing temperature, as listed in Fig. 2h, and this is a bit different from some co-workers' reports [2, 22, 23]. The average diameter of the grains was estimated by "Nano Measure1.2" software based on the SEM micrographs in our work. The average diameter of grains in the film decreased from ∼186 to ∼71 nm when the temperature increased from 650 to 750 °C, and the decrease of grain size with increasing temperature was possibly attributed to

volatilization of alkaline metal elements [17] or titanium diffusion from the substrate to the films at high temperature in all KNN films [24, 25]. The latter always happens at the grain boundaries, inhibiting the growth of the grain. The average diameter of the particles increased to ∼137 nm when the temperature was increased to 800 °C, which may be due to the suppression of the alkaline metal elements under the KNN atmosphere.

The cross-sectional SEM images (Fig. 2) show that KNN films annealed at 650 °C was crack-free and dense with thickness of approximately 200 nm. Whereas, the film annealed at 800 °C was porous and cracks, which may mainly result from the poor adhesion between KNN to Pt (100).

Figure 3 shows SEM images of the KNN films annealed in air at 650 and 800 °C, respectively. The KNN films annealed at 650 °C in air exhibited a relatively smooth surface with large grains size of ∼286 nm. When the temperature reached 800 °C, the grain size decreased to ∼72 nm. Figure 3c presents the diameter distribution of particles of KNN films annealed under different conditions, and the changing trend of average diameter of grains in the films annealed in air was very similar to that in the films annealed at the temperature range of 600–750 °C in KNN atmosphere while it is opposite to that in the films annealed in KNN atmosphere at the temperature range of 750–800 °C, which indicated that the KNN atmosphere has an obvious effect on promoting the grain growth in the

Fig. 3 SEM images of KNN films annealed at **a** 650 °C, **b** 800 °C in air and the average diameter of grains under different annealing conditions (**c**)
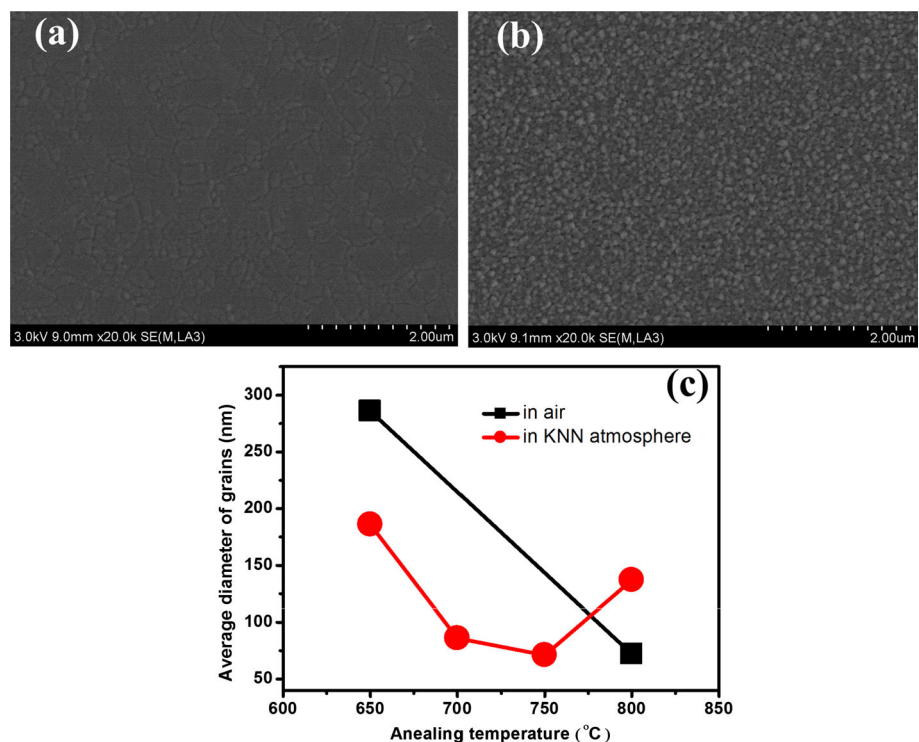
KNN films. Therefore, it's inferred that the grain size of KNN films strongly depended on the KNN atmosphere around 800 °C, while it was less affected below 800 °C.

The polarization–electric field ferroelectric hysteresis loops of KNN films measured at the frequency of 50 Hz with different annealing temperatures are presented in Fig. 4. The remnant polarization $2P_r$ and coercive field $2E_c$ values of the KNN films annealed at different temperatures are showed in Table 2. It can be seen that the KNN films annealed at 650 °C exhibited a desired remnant polarization with a high remnant polarization of $2P_r = 20.8$ μC/cm^2 and a coercive field $2E_c$ of 200 kV/cm under the electric field of about 550 kV/cm, which was related to the good crystallization, crystal orientation, large grain size and dense morphologies of the film. This $2P_r$ value was higher than the reported value of $2P_r = 16$ μC/cm^2 for RF-sputtered KNN films [26], and comparable to the value of $2P_r = 23.4$ μC/cm^2 reported by Bo-Yun Kim et al. [15]. The coercive field $2E_c$ of 200 kV/cm was much larger than that of only 80 kV/cm reported by Tao [26], which could be attributed to the better matched KNN/SRO interface than KNN/Pt/Ti/SiO$_2$/Si interface, in which domains could reverse much more easily.

Table 2 Remanent polarization and coercive field values of the KNN films annealed at different temperatures determined from the hysteresis measurements

Sample (°C)	$2P_r/(\mu C/cm^2)$	$2E_c/(kV/cm)$
600	–	–
650	20.28	200.25
700	4.59	93.75
750	2.95	42.5
800	2.92	60.25

The poor ferroelectric responses are detected in the case of annealing temperature ranging from 700 to 800 °C, which may result from the smaller grain size and porous morphology of the film annealed at higher temperatures. It has been suggested that the larger grains and the fewer grain boundaries in the films, the weaker the pinning or clamping effect of the domain walls became [27]. As we know, the ferroelectric properties depend on the domain switching. The smaller the domains, the higher the domain wall energy per volume ω_ω. However, the equilibrium size of domains is determined by a balance of energies (electrical field energy densities ω_e, mechanical field energies
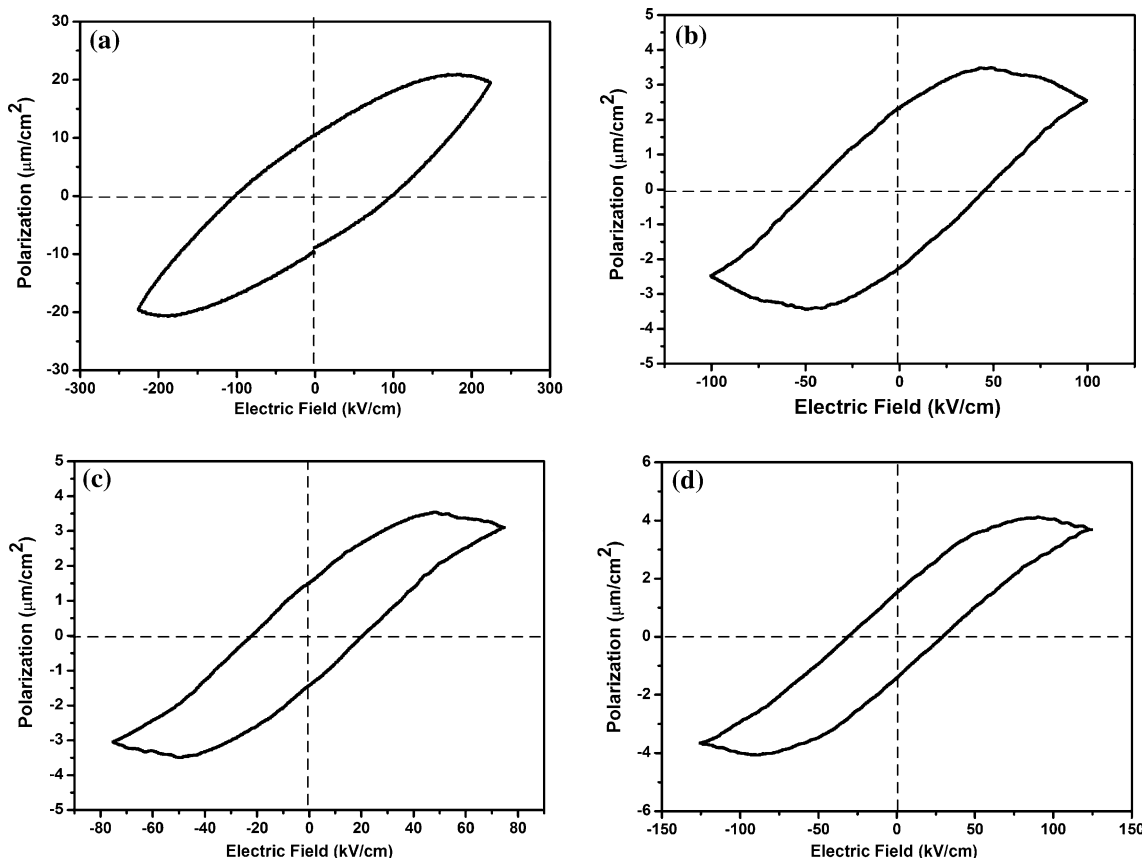

Fig. 4 Polarization-electric field ferroelectric hysteresis loops of KNN films with various annealing temperature: **a** 650 °C; **b** 700 °C; **c** 750 °C; **d** 800 °C
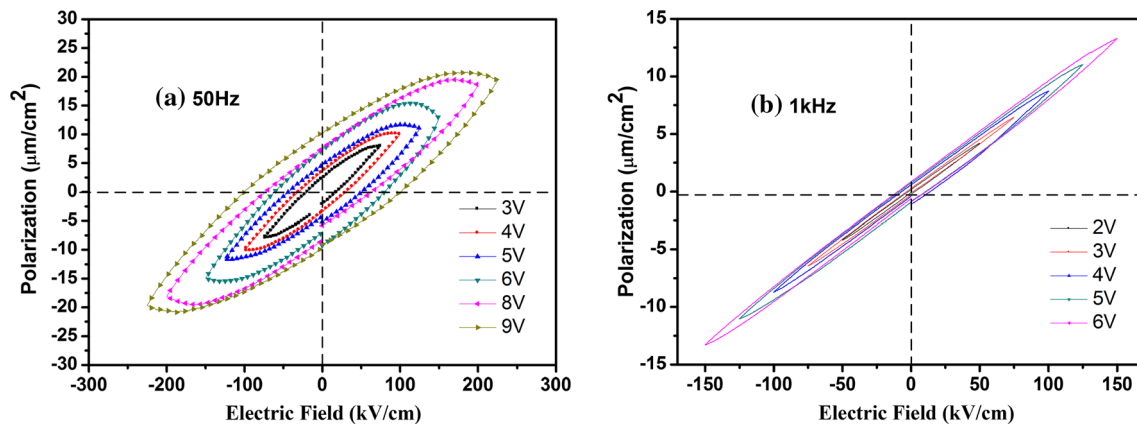
Fig. 5 Polarization–electric field ferroelectric hysteresis loops of KNN films annealed at 650 °C measured at different electric fields

ω_m and the domain wall energy ω_ω) [28]. The balance of three energies is given by:

$$minimum = \omega_e + \omega_m + \omega_\omega \tag{5}$$

Though the KNN films annealed at 800 °C exhibited the larger sizes than those annealed at 700 and 750 °C, it was porous and cracks as the cross-sectional morphology showed in Fig. 2h. It has been well known that when a high electric field is applied to the dielectric films, the pores in which will offer more leakage current paths, and increase the value of leakage current [29, 30].

Figure 5a and b shows the P–E loops of the KNN films annealed at 650 °C under 50 Hz and 1 kHz, respectively. The films measured at 50 Hz exhibited weak hysteresis loop at 3 V, and the shape and saturation of hysteresis loops at 8 and 9 V were improved, which are attributed to the switch polarization domains. However, the P–E loops measured at a frequency of 1 kHz present a long and thin shape, and had a lower breakdown field of 6 V compared with that of 9 V measured at 50 Hz. The frequency dependence of the polarizability can be similarly explained by the following equation proposed by Choong-Rae Chao et al. [31]:

$$f = \upsilon_{att} e^{-(UV_{act}/kT)}, \tag{6}$$

where υ_{att} is the attempt frequency, U is the height of the potential barrier, and V_{act} is the activation (polar cluster) volume. Choong-Rae Chao et al. [31] has pointed out that amounts of the polar clusters remain "frozen" below the Curie temperature, since it is not sufficient for the clusters to switch between equivalent polar states. When the temperature increases, more and more clusters begin to fluctuate between equivalent polar directions. In our study, the polarization–electric field (P–E) hysteresis loops were measured at room temperature, which is much below the Curie temperature. That is to say, only small amounts of clusters have a small activation volume. Therefore, increasing the measuring frequency would make it difficult for clusters to flip back and forth between equivalent polar directions, and thus leads to poor polarization at room temperature.

4 Conclusion

(Na, K)NbO₃ films were successfully obtained at 200 °C by RF magnetron sputtering deposition and subsequent annealing at different temperature under KNN atmosphere. XRD patterns show that the KNN films started crystallization accompanying with volatilization of alkaline elements as well as phase transition with increasing temperature. SEM images indicate that the diameter of particles and surface quality in the film depended on annealing temperature and atmosphere. The KNN films annealed at 650 °C exhibited a desired remnant polarization with $2P_r = 20.8$ μC/cm² and a coercive field $2E_c$ of 200 kV/cm under the electric field of about 550 kV/cm. The poor ferroelectric responses in higher temperature were due to the smaller grain sizes and porous morphology of the films. Meanwhile, frequencies and voltage both affected the shape and saturation of hysteresis loops for the film annealed at 650 °C.

References

1. A. Chowdhury, J. Bould, M.G.S. Londesborough, Mater. Chem. Phys. **124**, 159 (2010)
2. J. Ryu, J.J. Choi, B.D. Hahn, Appl. Phys. Lett. **90**, 152901 (2007)
3. P. Mahesh, S. Bashaiah, R.K.C. James, J. Am. Ceram. Soc. **98**, 1444 (2015)
4. H. Shiraki, S. Hirose, K. Kageyama, Jpn. J. Appl. Phys. **51**, 09LA05 (2012)

5. Q. Yu, J.F. Li, Y.N. Chen, J. Am. Ceram. Soc. **97**, 107 (2014)
6. S.Y. Lee, J.S. Kim, C.W. Ahn, Thin Solid Films **519**, 947 (2010)
7. G. Li, X.Q. Wu, W. Ren, Thin Solid Films **548**, 556 (2013)
8. P.C. Goh, K. Yao, Z. Chen, Appl. Phys. Lett. **99**, 092902 (2011)
9. F. Fu, B. Shen, J.W. Zhai, J. Alloys Compd. **509**, 7130 (2011)
10. A.F. Solarte, N. Pellegri, O. de Sanctics, J. Sol-Gel Sci. Technol. **66**, 488 (2013)
11. L.Y. Wang, W. Ren, P.C. Goh, Thin Solid Films **537**, 65 (2013)
12. G.F. Han, S. Priya, J. Ryu, Mater. Lett. **65**, 278 (2011)
13. N. Li, W.L. Li, L.D. Wang, J. Alloys Compd. **552**, 269 (2013)
14. N. Li, W.L. Li, L.D. Wang, Mater. Lett. **65**, 1010 (2011)
15. B.Y. Kim, T.G. Seong, I.T. Seo, Acta Mater. **60**, 3107 (2012)
16. P.C. Goh, K. Yao, Z. Chen, Appl. Phys. Lett. **97**, 102901 (2010)
17. K. Tanaka, K. Kakimoto, H. Ohsato, J. Cryst. Growth **294**, 209 (2006)
18. Q.L. Gu, K.J. Zhu, J.S. Liu, RSC Adv. **4**(29), 15104 (2014)
19. F. Fu, B. Shen, J.W. Zhai, Ceram. Int. **38S**, S287 (2012)
20. D.Y. Wang, D.M. Lin, K.W. Kwok, Appl. Phys. Lett. **98**, 022902 (2011)
21. L.Y. Wang, K. Yao, W. Ren, Appl. Phys. Lett. **93**, 092903 (2008)
22. A. Tian, W. Ren, L.Y. Wang, Appl. Surf. Sci. **258**, 2674 (2012)
23. X. Yan, W. Ren, X.Q. Wu, J. Alloys Compd. **508**, 129 (2010)
24. P.C. Goh, K. Yao, Z. Chen, J. Am. Ceram. Soc. **92**, 1322 (2009)
25. S. Wiegand, S. Flege, W. Ensinger, J. Sol-Gel Sci. Technol. **67**, 654 (2013)
26. T. Li, G.S. Wang, K. Li, Ceram. Int. **40**, 1195 (2014)
27. T. Lu, K.J. Zhu, J.S. Liu, J. Mater. Sci. Mater. Electron. **25**, 1112 (2014)
28. G. Arlt, D. Hennings, G. de With, J. Appl. Phys. **58**, 1619 (1985)
29. C.W. Ahn, S.Y. Lee, H.J. Lee, J. Phys. D Appl. Phys. **42**, 215304 (2009)
30. C.W. Ahn, E.D. Jeong, S.Y. Lee, Appl. Phys. Lett. **93**, 212905 (2008)
31. C.R. Cho, A. Grishin, J. Appl. Phys. **87**, 4439 (2000)